Effect of $CaCO_3$ Nanoparticles on Vibrational Damping Behavior and Static Mechanical Properties of Polypropylene Composite Plates: An Experimental Investigation

Mahdi Rahmani[1], Armen Adamian[2,] *, Ahmad Hosseini Sianaki[3]

Department of Mechanical Engineering,
Central Tehran Branch, Islamic Azad University, Tehran, Iran
E-mail: meh.rahmani.eng@iauctb.ac.ir, arm.adamian@iauctb.ac.ir,
a_h_sianaki@iauctb.ac.ir
*Corresponding author

Received: 23 June 2021, Revised: 28 October 2021, Accepted: 10 November 2021

Abstract: In this research, the effect of $CaCO_3$ nanoparticles was experimentally investigated on vibrational damping behavior and static mechanical properties of polypropylene (PP). Hammer tests along with modal analysis were carried out to evaluate the forced vibration behavior of composite plates under one edge clamped support conditions while tensile tests were performed to assess the static mechanical properties. A comparison of the results showed an increment in the static mechanical properties of nanocomposites by increasing the nanoparticles content in the PP matrix. Composite with 10 wt.% nanoparticles showed the highest rise in Young's modulus (39.71 %) compared to pure PP. An increment in Young's modulus and stiffness led to an increasing trend in the damped natural frequencies of the nanocomposites so that the composite with 10 wt. % nanoparticles showed the highest damped natural frequency augmentation (23.6 %, 36.78 %, and 252.62 %) compared to pure PP in the first three modes. In addition, an enhancement in the nanoparticles content of the PP matrix led to an increasing trend in damping ratios of the nanocomposites such that the composite with 10 wt. % nanoparticles in the first mode (28.99 %) and composite with 7.5 wt. % nanoparticles in the second and third modes (418.66 % and 9.93 %) showed the highest rise in damping ratio compared to pure PP. Increasing damping ratios can be due to the proper dispersion of nanoparticles in the matrix and consequently energy dissipation of the stick-slip mechanism between the matrix and nanoparticles. Moreover, high nanoparticle contents had destructive effects on both the static and dynamic behavior of the composites.

Keywords: Calcium carbonate nanoparticles, Forced vibration, Modal analysis, Nanocomposite.

How to cite this paper: Mahdi Rahmani, Armen Adamian, and Ahmad Hosseini Sianaki, "Effect of CaCO3 Nanoparticles on Vibrational Damping Behavior and Static Mechanical Properties of Polypropylene Composite Plates: An Experimental Investigation", Int J of Advanced Design and Manufacturing Technology, Vol. 15/No. 1, 2022, pp. 85–94.
DOI: 10.30495/admt.2022.1933897.1292.

Biographical notes: Mahdi Rahmani is a PhD student of Mechanical Engineering at the Central Tehran Branch, IAU, Tehran, Iran. He received his MSc in Mechanical Engineering from Shahid Rajaee Teacher Training University in 2012. **Armen Adamian** is an assistant professor of Mechanical Engineering at the Central Tehran Branch, IAU. He received his PhD in Mechanical Engineering from the University of California Los Angeles in 1986. His current research focuses on modal analysis, nanocomposites, structural dynamics. **Ahmad Hosseini-Sianaki** is an assistant professor of Mechanical Engineering at the Central Tehran Branch, IAU. He received his PhD in Mechanical Engineering from the University of Sussex, England in 1990. His current research focuses on vibration systems and applications of smart materials in engineering and biomechanics.

1 INTRODUCTION

Polypropylene (PP) has been extensively used as a thermoplastic material in diverse applications including automotive and packaging due to its low cost, lightweight, simple processing, and recyclability. Its low stiffness and impact strength due to the low glass transition temperature, however, has limited the applications of this polymer [1-2]. This problem has been addressed by compositing PP with nanoscale fillers [3-4]. In addition to their lighter weight, these composites offer better mechanical, thermal, and electrical properties [5]. Among mineral fillers, $CaCO_3$ nanoparticles (NPs) have been widely employed in the fabrication of polymer-based nanocomposites. Cost-effectiveness, availability, lightweight, ease of surface coating, facile preparation routes, and high load-bearing capacity are among the factors explaining the widespread use of this material as a reinforcement agent [6–8]. Thanks to their high surface-to-volume ratio, these nanoparticles can significantly increase Young's modulus, stiffness, and impact strength of the matrix upon proper interaction with the polymer substrate and uniform dispersion [9-10]. Nanocomposites prepared with single-layer coated $CaCO_3$ NPs provided the best mechanical properties (i.e. Young's modulus, tensile yield stress, and impact strength) due to proper dispersion of particles in the PP matrix. Energy dissipation in structures is another important issue in mechanical design to reduce the amplitude of vibrations. It is necessary to construct structural parts with a high level of mechanical damping. The levels of vibration during service or work should be predicted and controlled. In this regard, finding the dynamic characteristics of the structure is one of the fundamental parts of dynamic investigations. The modal analysis method could be a powerful tool in achieving this goal [11-12]. In modal analysis, it is important to determine three modal parameters: structural resonance frequencies to prevent the resonance, damping factor, and mode shapes to amplify points with maximum flexibility or determine suitable points for weight reduction or damping increase [13]. Polymer nanocomposites have provided an excellent opportunity to create new materials with high dynamic and mechanical capacity [14-15].

Manbari et al. [16] reported an improvement in the strength and toughness of PP due to the simultaneous presence of graphene and $CaCO_3$ NPs. Lin et al. [17] investigated the effect of coating and particle density on the impact toughness of PP/$CaCO_3$ nanocomposites. Chandradass et al. [18], theoretically and experimentally studied the free vibrations and damping properties of glass fiber-reinforced vinyl ester hybrid nanocomposites containing different weight percentages of nanoclay. Their results showed that the dispersion of the nanophase in the matrix and glass fibers significantly enhanced the internal damping of hybrid composites. Moreover, in previous experimental research, the vibrational behavior of nanocomposites has been mostly done by investigating the free vibrations of cantilever beams; However, in real conditions, structures are affected by forced vibrations and have more complex geometric shapes and are typically plate-shaped. Limited number of previous studies addressed the dynamic properties of polymer nanocomposites through forced vibration. Rafiei et al. [19] explored the forced vibration and damping properties of multi-layer fiberglass/epoxy composites modified with a wide range of carbon nanofillers for structural vibration applications. Experimental results showed that the damped natural frequency of nanocomposites increased with enhancing the particle density. At larger NPs contents, the damped natural frequencies decreased while the damping ratio increased.

Considering the positive effects of $CaCO_3$ NPs on the static mechanical properties of PP nanocomposites and significant effects of nano fillers on the dynamic behavior of polymer nanocomposites, the effect of different $CaCO_3$ NPs contents, morphology, and static mechanical properties on the vibrational behavior of PP nanocomposites was investigated to identify the forced vibration behavior of PP/$CaCO_3$ nanocomposites. Tensile tests were also employed to assess the static mechanical properties; while hammer tests with modal analysis were performed to examine the forced vibration behavior of polypropylene composite plates under one edge clamped support conditions. The results of mechanical tests were deductively studied and compared.

2 MATERIALS AND METHODS

2.1. Materials

In this research, polypropylene heterophase copolymer EPC40R with melt flow index of 7 g/10min was used (ASTM D 1238 / L @ 230 ˚C, 2.16 Kg, produced by Arak Petrochemical company of Iran). HAKUENKA CC-R $CaCO_3$ NPs with an average particle size of 80 nm and an initial stearic acid coating of 3.11 % (produced by Shiraishi-Omya GmbH, Austria) were used. Figures 1a and 1b show the FESEM image and powder of $CaCO_3$ NPs, respectively.

2.2. Sample Preparation

Pure PP and PP/ $CaCO_3$ nanocomposites were made under the same conditions through the physical mixing of the components. Before extruding the composites, $CaCO_3$ NPs were dried in an oven for 2 h at 120 °C. Composite ingredients (see “Table 1”) were mixed based on weight percentage.

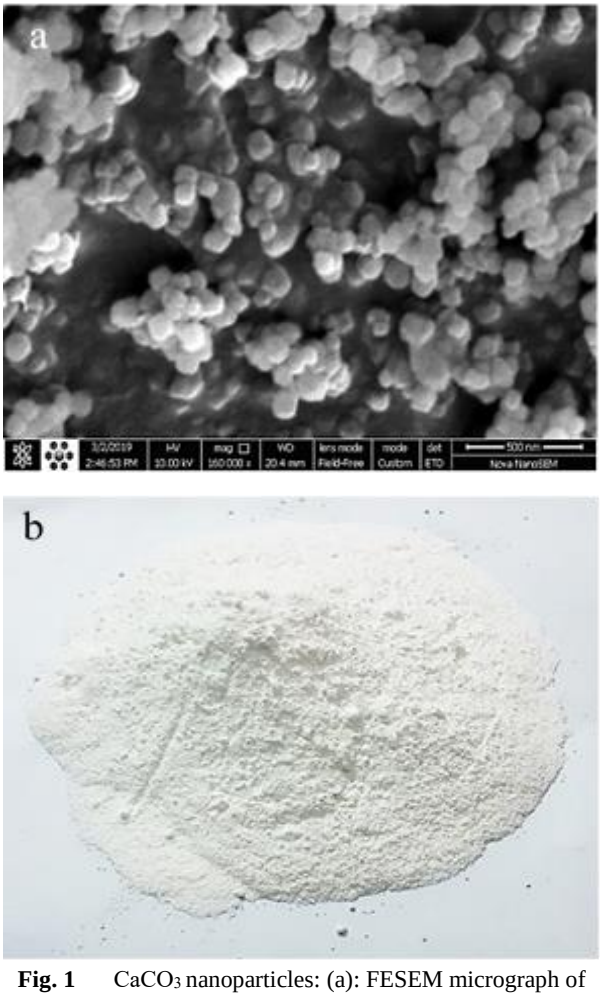

Fig. 1 $CaCO_3$ nanoparticles: (a): FESEM micrograph of CC-R at 160000 x magnification (Scalebar is 500 nm), and (b) $CaCO_3$ nanoparticles powder.

Table 1 Composite ingredients [a]

Abbreviation	Amounts of Component (wt.%)	
	PP	$CaCO_3$
PP	100.0	0
95P/5C	95.0	5.0
92.5P/7.5C	92.50	7.50
90P/10C	90.0	10.0
85P/15C	85.0	15.0

[a]Note: ''P'' and ''C'' denote Polypropylene and $CaCO_3$ in combination, respectively.

The materials were compounded using a co-rotating twin-screw extruder (ZSK 25 P 8.2 E WLE). Pure PP and blends were prepared with a temperature profile of 165/170/175/180/185/190 ˚C. The screw speed was set at 250 RPM. The L/D ratio of the screws was 40 and D = 25 mm.

The hot compounds were cooled down in a water bath and later granulated and hot-pressed into square plates for vibration test. Hot-pressing was carried out at 210 ˚C and 50 MPa for 30 min using Koosha hydraulic hot press machine. The samples were cooled under a pressure of 25 MPa using water flow for 30 min (Toyoseikei mechanical cold-press machine).

All tensile test specimens were molded in dumbbell shapes with the dimension of 150×20×4 mm^3 according to ISO 527 Type / standard and all vibration test specimens were made as square plates with a dimension of 160×160×1.5 mm^3. All composite plates were meshed at 20×20 mm^2 to determine the exact points of force application and installation of the vibration system response sensor.

Figure 2a shows a meshed composite plate specimen on which the order of points to receive a hammer force is specified which was determined by the vibration test software. A suitable support frame was also designed and fabricated to create one edge clamped boundary conditions on the composite plates in the vibration test, see "Fig. 2b".

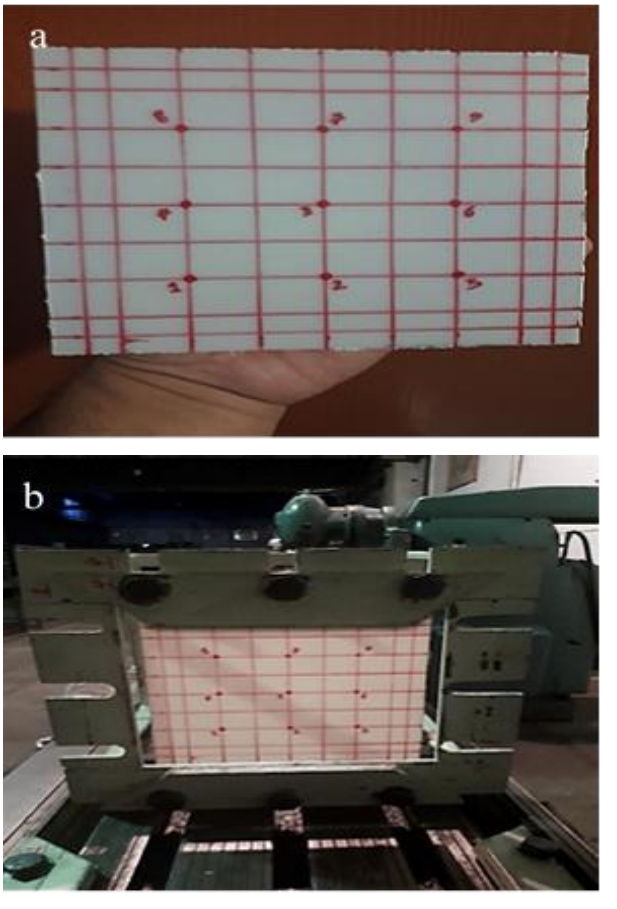

Fig. 2 Vibration test plate: (a): meshed plate, (b): plate with one edge clamped support condition (CFFF).

2.3. Scanning Electron Microscopy and Phase Structure Analysis

A Field Emission Scanning Electron Microscope (FESEM) was employed to assess the composites microstructure and particles dispersion and size using an FEI NOVA NANOSEM 450 microscope working at 10 kV. The specimens were obtained by cryogenic fracture. After immersing the sample in liquid nitrogen for more than 20 min, it was immediately broken by hand (less than 3 s). The SEM samples were coated using a sputter coater (Quorum Q 150 T ES PVD, for 12 min at 6 kV and 5 mA flow; under argon gas atmosphere) by a thin film of gold to prevent electrical charge accumulation.

2.4. Mechanical Tests

Tensile tests were performed at room temperature (23 ^{o}C) using an Instron 5566 testing machine, according to ISO 527 Type I standard to obtain stress-strain data. A constant crosshead speed of 5 mm/min was used in the tensile tests. Young's modulus was calculated within the linear range of the tensile stress-strain curves in the strain interval of 0.05 % to 0.25 % according to Hook's law. The average value of the tensile properties was calculated considering at least five samples.

The hammer test and modal analysis were utilized to extract the natural frequency and damping ratio and examine the effect of components on the forced vibration behavior under one edge clamped boundary conditions. The hammer test is a popular test for the investigation of the vibration behavior of composite plates [20]. To stimulate the composite plates at the specified points and create forced vibration conditions, an IH-02 model hammer of DJB instruments with 2.5 mV/N sensitivity and 80 g head weight was used to apply the force. The data were collected by a piezoelectric force transducer (YMC company; model: 512F02) connected to the hammer head as well as channel 4 of the analyzer.

An accelerometer (Globaltest company; model: AP 2030-10) with 1 mV/m/s² sensitivity and 2 g weight connected to channel 1 of the analyzer was employed to receive the vibration response of the plates. Due to the low weight of the accelerometer and the effects of sensor displacement on the output response, this sensor was connected to the back of the plate by wax on node 1. Different nodes were stimulated by the hammer.

Figure 3a"schematically shows the device set-up. Each composite plate was tested considering the one edge clamped support conditions. Based on the meshing of the plates, 9 specified nodes were continuously hit by the hammer using a random load. Acceleration and force signals were collected and amplified using a 3160-A-042 Bruel & Kjær analyzer and the corresponding responses were stored on a computer. Bruel and Kjaer connect 2018 software was used to perform the tests and analyze the results.

Initial test settings included: baseband analysis mode, frequency span up to 3200 Hz (FFT Lines = 3200), the frequency resolution of 1 Hz, averaging time of 0.6667 s, linear averaging, and the number of averages was 1000 samples per second. Two channels of Fast Fourier Transform (FFT) analysis of the system input and output made it possible to calculate the transfer function (TF), which describes the dynamic behavior of the plate, assuming a linear system.

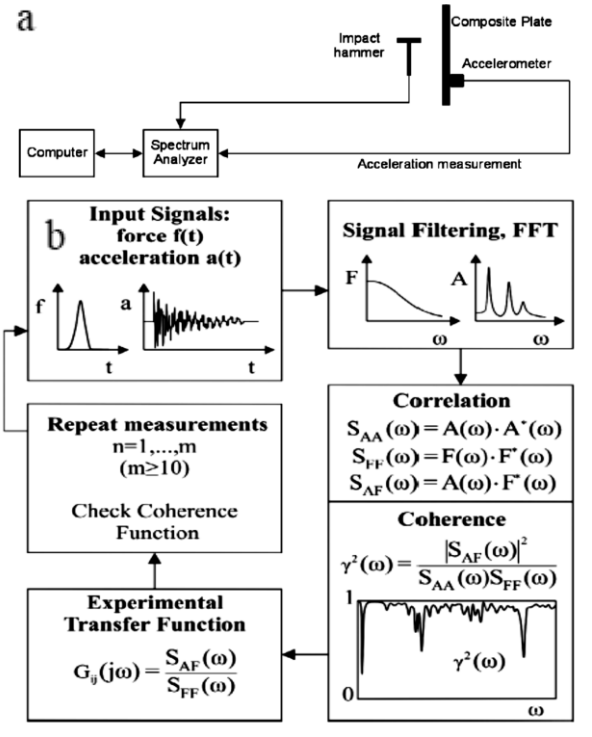

Fig. 3 Schematic diagram of modal analysis: (a): device connection for the hammer test, and (b): The signal processing procedure of the vibration tests: autospectra of force, S_{FF}, and acceleration, S_{AA}, cross-spectrum S_{AF} (where* indicates complex conjugation), coherence function evaluation, and the averaged transfer function of the measurements [21].

The signal processing procedure for the vibration tests is shown in "Fig. 3b". The response to the excitation function ratio was calculated to obtain corresponding transfer function modes. The response can be calculated in different ways such as displacement, velocity, or acceleration, thus, different components can be considered for force-to-response ratios [21]. In this study, the acceptable transfer function for each node and its FRF diagram were extracted by measuring the displacement using the accelerometer and calculating the displacement ratio of the excitation to the applied force. Finally, by matching the FRF diagrams of all 9 nodes in the specified frequency range, different vibration modes of the plates were identified considering

the peak points of the FRF diagram (peak picking (PP) technique). Natural frequencies and damping ratio of each plate were extracted under the one edge clamped support conditions in the range of 0-800 Hz. The software suggested the multi-degree of freedom systems (MDOF) of polyreference time (PTD) curve-fitting method and the advanced rational fraction polynomial-Z (RFP-Z) modal analysis method. The same method was employed to compute the natural frequencies and damping ratio with data consistency settings in global solve mode and maximum iterations of 200.

3 RESULTS AND DISCUSSION

3.1. Structural Characteristics of The Composites

Figures 4a to 4e show the FESEM images taken from the broken surfaces of PP nanocomposites filled with 5, 7.5, 10, and 15 wt.% $CaCO_3$ NPs and pure PP, respectively. As seen, at all filler contents, the particles exhibited a good dispersion as their surface modification by stearic acid significantly reduced the free surface energy of the filler, hence, declining the particle-particle interactions [17]. However, in the composite with 15 wt.% $CaCO_3$ NPs ("Fig. 4d"), the particle dispersion slightly decreased giving rise to little agglomeration. At high particle contents, the distance between the particles decreased; raising the possibility of interparticle interactions, thereby, their agglomeration. Although the coating process significantly reduced the surface energy, particle agglomeration is probable at high filler contents due to the small size of the particles, their high specific surface area, and free surface energy [9].

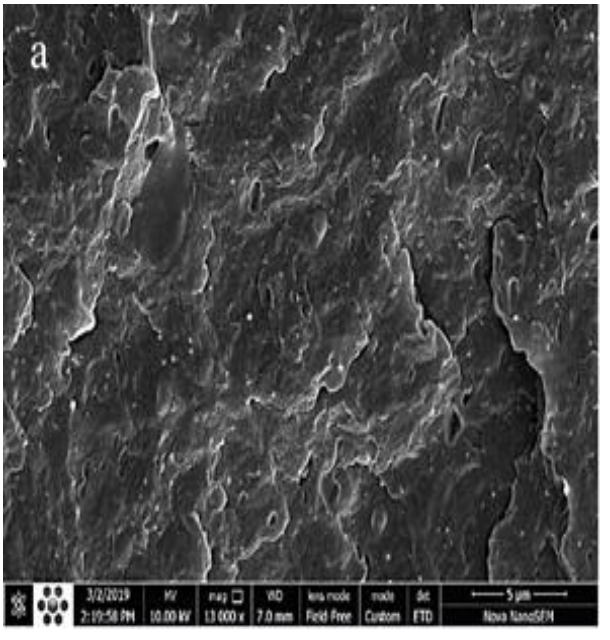

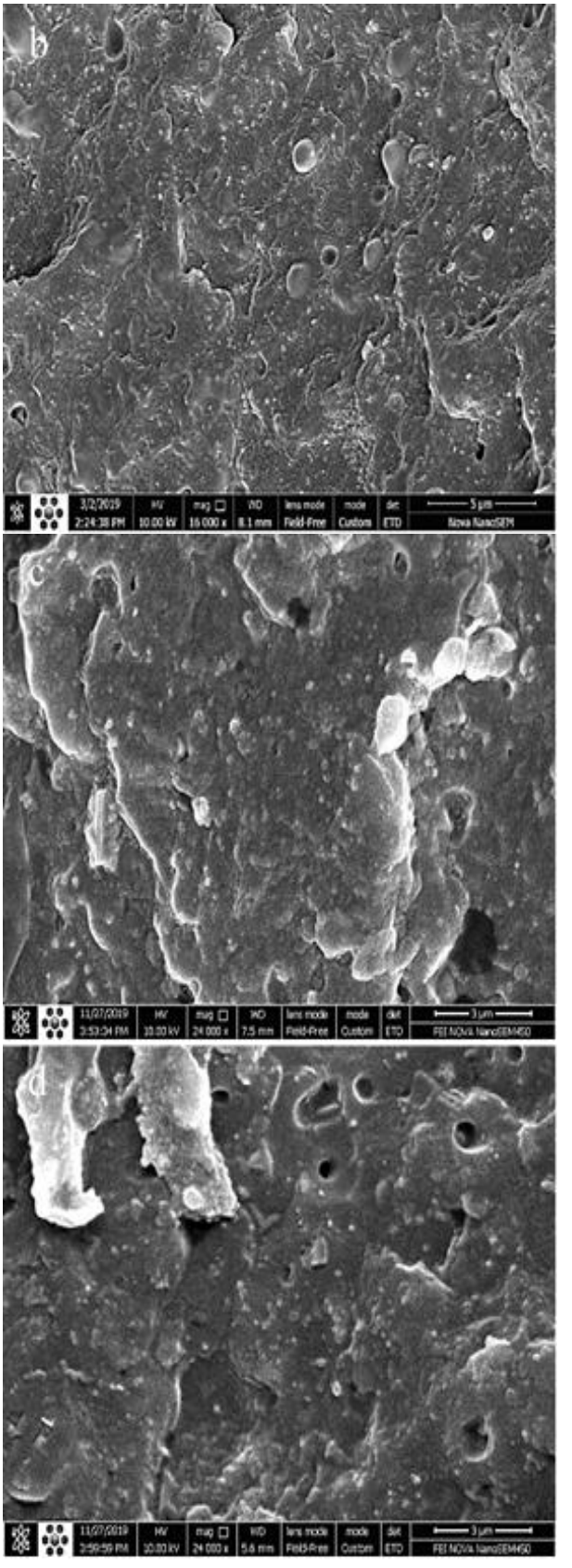

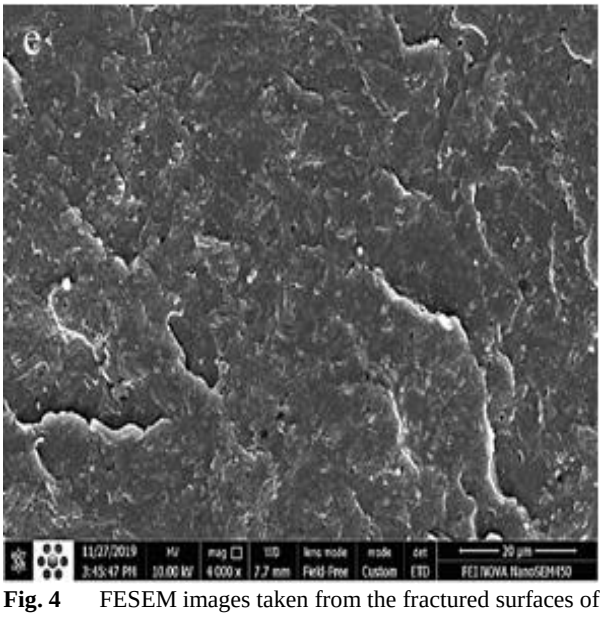

Fig. 4 FESEM images taken from the fractured surfaces of nanocomposites: (a): PP/5C, (b): PP/7.5C, (c): PP/10C, (d): PP/15C, and (e): PP.

3.2. Experimental Analysis of Static Mechanical Properties and Vibrational Damping Behavior

3.2.1. Effect of $CaCO_3$ NPs on the Static Mechanical Properties of Polypropylene

Figure 5 shows yield stress, tensile strength, and elongation at break of pure PP and PP/$CaCO_3$ composites containing different levels of $CaCO_3$ NPs. The error bars in each column of the graph show the maximum deviation from the average results of the experiment. As it can be seen, the yield stress and tensile strength of the PP/$CaCO_3$ nanocomposites showed an increasing trend with elevating the filler content which can be assigned to the strong interaction between $CaCO_3$ NPs and PP matrix [6], [9], [17]. Although the yield stress of all composites was higher than that of pure polypropylene, the yield stress of composites containing higher contents of nanoparticles did not exhibit a significant difference. In the composite containing 15 wt.% $CaCO_3$ NPs, a reduction occurred in yield stress. The destructive effects of high NPs contents on the ultimate tensile strength were also observed such that beyond 10 wt.% NPs, the tensile strength was decreased due to the agglomeration of $CaCO_3$ NPs as a result of their high surface energy, leading to premature separation of the particles from the matrix.

The elongation at break of the composites also exhibited a gradual decrement by increasing the content of $CaCO_3$ NPs. At higher filler levels, more particles will be separated from the matrix, leading to premature fracture of the material. On the other hand, the particles can serve as nucleation centers and reduce the mobility of polymer chains by creating a kinetic barrier, giving rise to the formation of small and incomplete crystals which can enhance the matrix crystallinity. Such an internal crystallization can be formed in polymers by crystallization of the particles on the surface. In the case of PP, the inner crystalline layer showed higher stiffness and lower deformability [6-7].

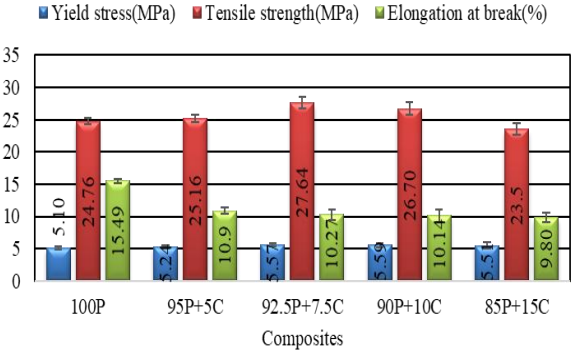

Fig. 5 Yield stress, tensile strength, and elongation at break of pure PP and PP/$CaCO_3$ nanocomposite containing different weight percentages of $CaCO_3$ NPs.

Figure 6 shows Young's modulus of pure PP and PP/$CaCO_3$ composites containing different levels of $CaCO_3$ NPs.

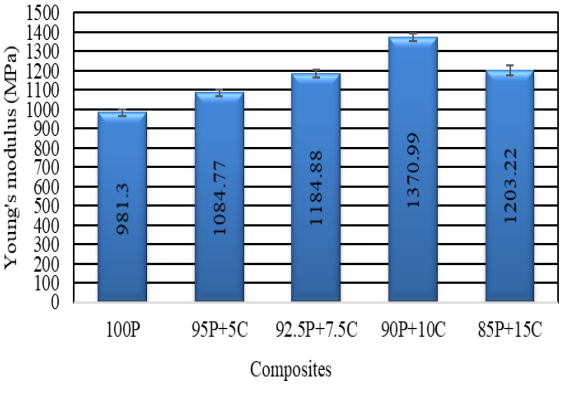

Fig. 6 Young's modulus of pure PP and PP/$CaCO_3$ nanocomposite with different $CaCO_3$ contents.

As seen, the incorporation of rigid nanoparticles into the PP matrix increased Young's modulus. Such an increment in Young's modulus, in addition to the stiffness of $CaCO_3$ NPs, could be due to the inseparability of nanoparticles from the matrix in the elastic region during the tensile test [7], [21]. The rise in modulus of the elastic region prior to the particle separation indicates a proper particle-matrix adhesion at low strain rates [9], [17]. The highest increase (39.71 %) in Young's modulus compared to pure PP occurred in the composite containing 10 wt.% $CaCO_3$ NPs. Young's modulus showed a decline in the case of PP/$CaCO_3$ composite with 15 wt.% NPs which can be attributed to the agglomeration of nanoparticles. As previously

reported [6], [22], $CaCO_3$ NPs can act as a nucleation center in the PP matrix. By reducing the size of spherulites and creating a kinetic barrier, the mobility of polymer chains and the amorphous phase of PP decreased leading to the formation of small and imperfect crystals and ultimately the rise in the matrix crystallinity. The influence of the secondary phase on polymeric materials depends on the crystallization of the polymer. This internal crystallization can initiate by the crystallization from the particle surface. In the case of PP, the inner crystalline layer exhibited a higher stiffness and lower deformation, thus, enhancing Young's modulus of the composite. It was shown that the incorporation of $CaCO_3$ NPs in a polypropylene matrix can decrease the brittle-to-ductile transition temperature and increase the elastic modulus compared to a pure polymer matrix [2].

3.2.2. Effect of $CaCO_3$ NPs on the Vibration Behavior of Polypropylene

Figure 7 shows the damped natural frequency of the first three modes for pure PP and PP/$CaCO_3$ nanocomposites containing different contents of $CaCO_3$ NPs under one edge clamped support conditions. As it can be seen, an increase in the content of $CaCO_3$ NPs augmented the frequency of composites in all three modes.

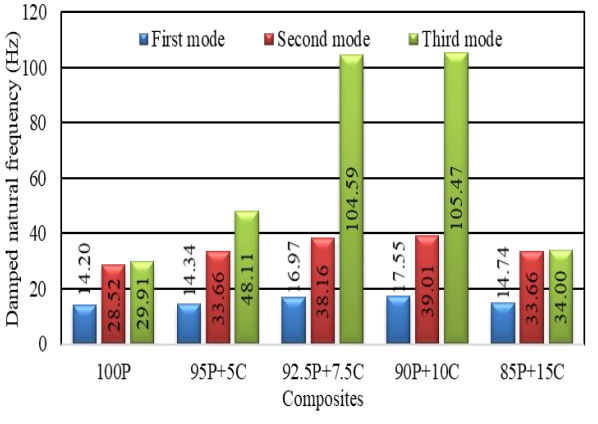

Fig. 7 Damped natural frequency of the first three modes of pure PP and PP/$CaCO_3$ composite plates containing different contents of $CaCO_3$ NPs under one edge clamped support conditions.

The composite containing 10 wt. % $CaCO_3$ NPs showed the highest frequency increase compared to pure PP. First, second, and third frequencies for this composite also exhibited 23.6 %, 36.78 %, and 252.62 % increase compared to those of pure PP, respectively. These values also suggested more variations due to the presence of $CaCO_3$ NPs at higher frequencies. The natural frequency is directly related to Young's modulus and inversely to the mass of the element [21], [23]. Therefore, the enhancement in the frequency of composites by raising the $CaCO_3$ NPs content could be due to the increment in Young's modulus and stiffness of the composites in the presence of NPs where high Young's modulus coincided with slight changes in the mass of the composites due to NPs incorporation [19], [23-24]. Balaganesan et al. [25] observed similar results and reported a significant increase in the natural frequency of nanocomposites filled with clay nanoparticles compared to the pure matrix by elevating the content of NPs to 3 wt. %. The sample containing 15 wt.% $CaCO_3$ NPs showed a decrease in frequency due to the agglomerations of $CaCO_3$ NPs leading to the destruction of Young's modulus and stiffness, hence, a reduction in the frequency of composite [18], [26-27].

Figure 8 shows the damping ratio of the first three modes for pure PP and PP/$CaCO_3$ nanocomposites containing different levels of $CaCO_3$ with one edge clamped support. As it can be seen, an increase in the weight percentage of $CaCO_3$ NPs raised the damping ratio of the composites in all three modes.

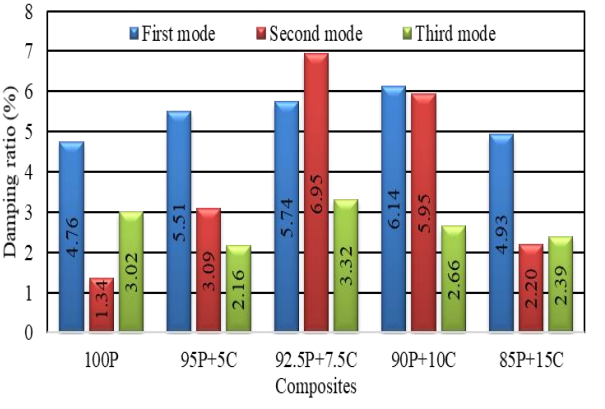

Fig. 8 Damping ratio of the first three modes for pure PP and PP/$CaCO_3$ composite plates containing different levels of $CaCO_3$ NPs under one edge clamped support conditions.

The composite containing 10 wt. % $CaCO_3$ NPs showed the highest increase (28.99 %) in the damping ratio in the first mode compared to pure PP while the composite with 7.5 wt. % $CaCO_3$ NPs exhibited the highest increase in damping ratio in the second and third modes (418.66 % and 9.93 %, respectively). The reason could be the increase in energy dissipation due to the stick-slip mechanism between the matrix and $CaCO_3$ NPs and also the reduction of polymer matrix cross-link due to the presence of nanoparticles. Nanoparticles can serve as a nucleation site and reduce the mobility of polymer chains by creating a kinetic barrier, leading to the formation of small and imperfect crystals, thereby, increasing the crystallinity of the matrix and damping [21], [28]. Moreover, under uniaxial stress, the nanoparticles may act as focal stress points; thus, the matrix and the particle strain will be equal until the interfacial shear stress reaches its critical value. At this stage, the particle will separate from the matrix and the

matrix will slip on it, leading to energy dissipation [7], [28].

In fact, the large stiffness difference between the filler particles and the matrix increased the interlayer stresses at the particle-matrix interface, interlayer shear strength, and internal damping, and as a result, the total damping [18]. Thanks to their high surface-to-volume ratio, $CaCO_3$ NPs can establish proper bonds with the PP matrix. Under vibration, these bonds may act as energy dissipation points, giving rise to energy loss in the form of heat and further increasing the damping ratio of the composites [23].

Despite the higher damping ratio of PP/$CaCO_3$ 15 wt.% than pure PP, it exhibited a lower damping ratio compared to other composites with lower NPs content. Such an observation can be due to the agglomerations of nanoparticles at high contents of $CaCO_3$ NPs which decreased the contact surface of the particles with the matrix and consequently reduced the energy dissipation of the composite. The dispersion of nanoparticles in the matrix also affected the energy dissipation, and therefore, the damping. The agglomeration of nanoparticles reduced the active area in the interfacial slip, giving rise to a decline in dissipated energy [18], [24].

3.2.3. Mode Shape Changes

Figure 9 shows the mode shapes of the first three modes for pure PP and PP/$CaCO_3$ nanocomposites containing different $CaCO_3$ contents with one edge clamped support. The mode shapes were investigated by comparing the composites with the pure PP [29]. As it can be seen, the composites containing 5 and 7.5 wt. % $CaCO_3$ NPs showed the mode shapes similar to pure PP and the addition of nanoparticles up to 7.5 wt. % did not significantly alter the mode shapes of the composites, especially in the first mode [30].

In the first mode, the mode shape of the composites with a small content of nanoparticles was the 1st bending around the X-axis [12], [31]. Hosseini Farrash et al. [28] also reported similar results for the first mode shapes of the CNT-filled epoxy composites plates under one edge clamped support conditions. However, the binary composite containing 10 and 15 wt.% $CaCO_3$ NPs showed different and irregular mode shapes compared to the composites with lower nanoparticle contents. As confirmed before, particle agglomeration can result in irregularities in the mode shapes [32-33]. In the first mode, this composite showed the 2nd bending around the X-axis. This irregularity is especially noticeable in the first mode. Herman et al. [34] also examined the modal analysis of defect vibrations in composite T-plates and declared that the lower-order mode shapes are more reliable indicators of damage while higher-order modes are less susceptible to the presence of damage.

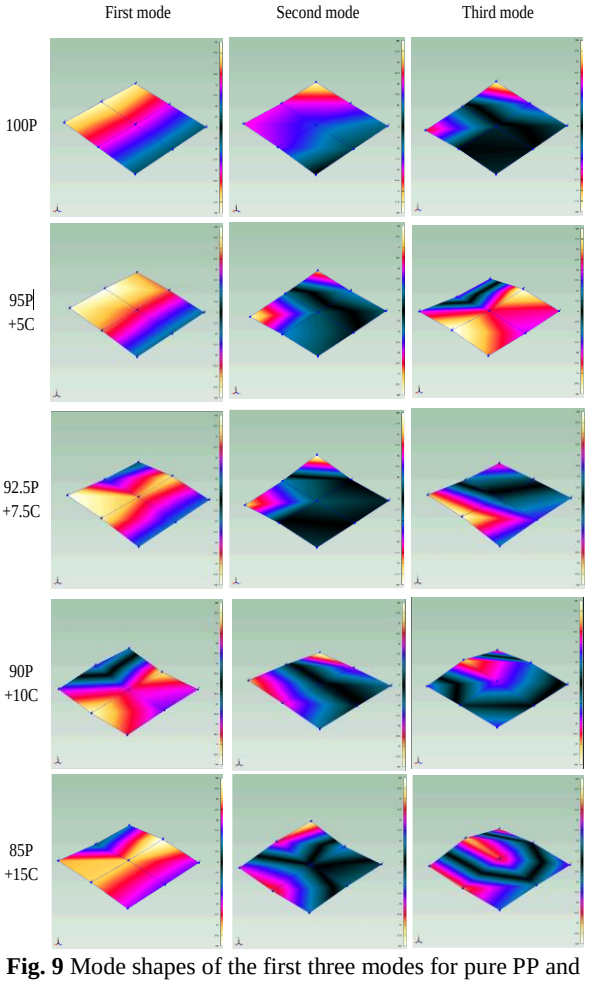

Fig. 9 Mode shapes of the first three modes for pure PP and PP/$CaCO_3$ plates containing different contents of $CaCO_3$ NPs with one edge clamped support conditions.

4 CONCLUSION

In this research, the effect of $CaCO_3$ NPs on vibrational damping behavior and static mechanical properties of PP was experimentally assessed. The tensile test was performed to investigate static mechanical properties while the forced vibration behavior of PP was evaluated by the hammer test under the one edge clamped (CFFF) support condition. The most important results of this research can be summarized as:

- Despite the proper NPs dispersion in the binary composites up to 10 wt.%, the composite containing 15 wt.% NPs showed the slightly reduced quality of dispersion due to agglomeration which destructively affected both vibrational damping behavior and static mechanical properties of the composites.

-Yield stress, tensile strength, and Young's modulus of the PP/$CaCO_3$ nanocomposites showed an increasing trend by enhancing the filler content due to the strong interaction between $CaCO_3$ NPs and PP matrix and the

reinforcement of the matrix by these particles. The highest increase in Young's modulus (39.71 %) was observed in the sample containing 10 wt. % $CaCO_3$ NPs.
-All the damped natural frequencies of the composites in the first three modes exhibited an increasing trend upon elevating the content of nanoparticles in the PP matrix due to the increase in Young's modulus and the stiffness. The composite with 10 wt.% $CaCO_3$ NPs showed the highest damped natural frequency increase compared to pure PP with 23.6 %, 36.78 %, and 252.62 % in the first to third modes, respectively.
-All the damping ratios of the composites in the first three modes showed an enhancement with increasing the weight percentage of nanoparticles due to energy dissipation of the stick-slip mechanism between the matrix and nanoparticles. The highest damping ratio increase compared to pure PP was detected in composite with 10 wt.% $CaCO_3$ NPs, in the first mode (28.99 %), and composite with 7.5 wt. % $CaCO_3$ NPs, in the second and third modes (418.66 % and 9.93 %).
-In the first and second modes, the composites containing 5 and 7.5 wt. % $CaCO_3$ NPs showed mode shapes similar to those of pure PP. The incorporation of NPs does not significantly alter the mode shape of the composite, especially in the first mode. However, the binary composites containing 10 and 15 wt.% $CaCO_3$ NPs exhibited different mode shapes with irregularities due to the agglomeration of NPs.

DECLARATIONS

•Funding
The funding sponsors had no role in the design of the study; in the collection, analyses, or interpretation of data; in the writing of the manuscript, and in the decision to publish the results

•Conflicts of interests
The authors declare no conflicts of interest.

REFERENCES

[1] Bakhtiari, A., Ghasemi, F. A., Naderi, G., and Nakhaei, M. R., An Approach to the Optimization of Mechanical Properties of Polypropylene/Nitrile Butadiene Rubber/Halloysite Nanotube/Polypropylene-g-Maleic Anhydride Nanocomposites Using Response Surface Methodology, Polymer Composites, Vol. 41, No. 6, 2020, pp. 1–14, DOI: 10.1002/pc.25541.

[2] Eiras, D., Pessan, L. A., Mechanical Properties of Polypropylene/Calcium Carbonate Nanocomposites, Materials Research, Vol. 12, No. 4, 2009, pp. 517–522, DOI: 10.1590/S1516-14392009000400023.

[3] Ke, F., Jiang, X., Xu, H., Ji, J., and Su, Y., Ternary Nano-$CaCO_3$/Poly (Ethylene Terephthalate) Fiber/Polypropylene Composites: Increased Impact Strength and Reinforcing Mechanism, Composites Science and Technology, Vol. 72, No. 5, 2012, pp. 574–579, DOI: 10.1016/j.compscitech.2012.01.001.

[4] Kiran, M. D., Govindaraju, H. K., Jayaraju T., and Kumar, N., Effect of Fillers on Mechanical Properties of Polymer Matrix Composites, Materials Today: Proceedings, Vol. 5, No 10, 2018, pp. 22421–22424, DOI: 10.1016/j.matpr.2018.06.611.

[5] Yetgin, S. H., Effect of Multi Walled Carbon Nanotube on Mechanical, Thermal and Rheological Properties of Polypropylene, Journal of Materials Research and Technology, Vol. 8, No. 5, 2019, pp. 4725–4735, DOI: 10.1016/j.jmrt.2019.08.018.

[6] Nascimento, E. M., Eiras, D., and Pessan, L. A., Effect of Thermal Treatment on Impact Resistance and Mechanical Properties of Polypropylene/Calcium Carbonate Nanocomposites, Composites Part B, Vol. 91, 2016, pp. 228–234, DOI: 10.1016/j.compositesb.2015.12.040.

[7] Lapcik, L., Manas, D., Vasina, M., Lapcikova, B., Reznicek, M., and Zadrapa, P., High Density Poly (Ethylene)/$CaCO_3$ Hollow Spheres Composites for Technical Applications, Composites Part B, Vol. 113, 2017, pp. 218–224, DOI: 10.1016/j.compositesb.2017.01.025.

[8] Palanikumar, K., AshokGandhi, R., Raghunath, B. K., and Jayaseelan, V., Role of Calcium Carbonate ($CaCO_3$) in Improving Wear Resistance of Polypropylene (PP) Components Used in Automobiles, Materials Today: Proceedings, Vol. 16, No. 2, 2019, pp. 1363–1371, DOI: 10.1016/j.matpr.2019.05.237.

[9] Lam, T. D., Hoang, T. V., Quang, D. T., and Kim, J. S., Effect of Nanosized and Surface-Modified Precipitated Calcium Carbonate on Properties of $CaCO_3$/Polypropylene Nanocomposites, Materials Science and Engineering A, Vol. 501, No. 1, 2009, pp. 87–93, DOI: 10.1016/j.msea.2008.09.060.

[10] Ghari, H. S., Jalali-Arani, A., Nanocomposites Based on Natural Rubber, Organoclay and Nano-Calcium Carbonate: Study on the Structure, Cure Behavior, Static and Dynamic-Mechanical Properties, Applied Clay Science, Vol. 119, No. 2, 2016, pp. 348–357, DOI: 10.1016/j.clay.2015.11.001.

[11] Rajeshkumar, G., Hariharan, V., Free Vibration Characteristics of Phoenix Sp Fiber Reinforced Polymer Matrix Composite Beams, Procedia Engineering, Vol. 97, 2014, pp. 687–693. DOI: 10.1016/j.proeng.2014.12.298.

[12] Cakir, F., Uysal, H., and Acar, V., Experimental Modal Analysis of Masonry Arches Strengthened with Graphene Nanoplatelets Reinforced Prepreg Composites, Measurement, Vol. 90, 2016, pp. 233–241, DOI: 10.1016/j.measurement.2016.04.061.

[13] Mansour, G., Tsongas, K., and Tzetzis, D., Investigation of the Dynamic Mechanical Properties of Epoxy Resins Modified with Elastomers, Composites Part B, Vol. 94, 2016, pp. 152–159, DOI: 10.1016/j.compositesb.2016.03.024.

[14] Treviso, A., Genechten, B. V., Mundo, D., and Tournour, M., Damping in Composite Materials: Properties and Models, Composites Part B, Vol. 78, 2015, pp. 144–152, DOI: 10.1016/j.compositesb.2015.03.081.

[15] Prasob, P. A., Sasikumar, M., Static and Dynamic Behavior of Jute/Epoxy Composites with ZnO and TiO_2 Fillers at Different Temperature Conditions, Polymer Testing, Vol. 69, 2018, pp. 52–62, DOI: 10.1016/j.polymertesting.2018.04.040.

[16] Menbari, S., Ghasemi, F. A., and Ghasemi, I., Simultaneous Improvement in the Strength and Toughness of Polypropylene by Incorporating Hybrid Graphene/$CaCO_3$ Reinforcement, Polymer Testing, Vol. 54, 2016, pp. 281–287, DOI: 10.1016/j.polymertesting.2016.07.026.

[17] Lin, Y., Chen, H., Chan, C. M., and Wu, J., Effects of Coating Amount and Particle Concentration on the Impact Toughness of Polypropylene/$CaCO_3$ Nanocomposites, European Polymer Journal, Vol. 47, No. 3, 2011, pp. 294–304, DOI: 10.1016/j.eurpolymj.2010.12.004.

[18] Chandradass, J., Kumar, M. R., and Velmurugan, R., Effect of Nanoclay Addition on Vibration Properties of Glass Fibre Reinforced Vinyl Ester Composites, Materials Letters, Vol. 61, No. 22, 2007, pp. 4385–4388, DOI: 10.1016/j.matlet.2007.02.009.

[19] Rafiee, M., Nitzsche, F., and Labrosse, M. R., Fabrication and Experimental Evaluation of Vibration and Damping in Multiscale Graphene/Fiberglass/Epoxy Composites, Journal of Composite Materials, Vol. 53, No. 15, 2019, pp. 2105–2118, DOI: 10.1177/0021998318822708.

[20] Arumugaprabu, V., Uthayakumar, M., Manikandan, V., Rajini, N., and Jeyaraj, P., Influence of Redmud on the Mechanical, Damping and Chemical Resistance Properties of Banana/Polyester Hybrid Composites, Materials & Design, Vol. 64, 2014, pp. 270–279, DOI: 10.1016/j.matdes.2014.07.020.

[21] Mansour, G., Tsongas, K., and Tzetzis, D., Modal Testing of Nanocomposite Materials Through an Optimization Algorithm, Measurement, Vol. 91, 2016, pp. 31–38, DOI: 10.1016/j.measurement.2016.05.032.

[22] Eiras, D., Pessan, L. A., Influence of Calcium Carbonate Nanoparticles on the Crystallization of Olypropylene, Materials Research, Vol. 12, No. 4, 2009, pp. 523–527, DOI: 10.1590/S1516-14392009000400024.

[23] Vibratory Behaviour of Glass Fibre Reinforced Polymer (GFRP) Interleaved with Nylon Nanofibers, Composite Structures, Vol. 176, 2017, pp. 923–932, DOI: 10.1016/j.compstruct.2017.06.018.

[24] Mohan, T. P., Velmurugan, R., and Kanny, K., Damping Characteristics of Nanoclay Filled Hybrid Laminates During Medium Velocity Impact, Composites Part B, Vol. 82, 2015, pp. 178–189, DOI: 10.1016/j.compositesb.2015.08.016.

[25] Balaganesan, G., Velmurugan, R., Vibration and Energy Dissipation of Nanocomposite Laminates for Below Ballistic Impact Loading, Latin American Journal of Solids and Structures, Vol. 12, No. 12, 2015, pp. 2259–2280, DOI: 10.1590/1679-78251703.

[26] Pei, X., Chen, L., Li, J., Tang, Y., and Chen, K., Effect of Damage on the Vibration Modal of a Novel Three-Dimensional and Four-Directional Braided Composite T-Beam, Composites Part B, Vol. 86, 2016, pp. 108–119, DOI: 10.1016/j.compositesb.2015.09.022.

[27] Kordani, N., Fereidoon, A., and Ashoori, M., Damping Augmentation of Nanocomposites Using Carbon Nanotube/Epoxy, Structural Dynamics, Vol. 3, 2011, pp. 1605–1615, DOI: 10.1007/978-1-4419-9834-7_145.

[28] Farrash, S. M. H., Shariati, M., and Rezaeepazhand, J., The Effect of Carbon Nanotube Dispersion on the Dynamic Characteristics of Unidirectional Hybrid Composites: An Experimental Approach, Composites Part B, Vol. 122, 2017, pp. 1–8, DOI: 10.1016/j.compositesb.2017.04.003.

[29] Heshmati, M., Yas, M. H., and Daneshmand, F., A Comprehensive Study on the Vibrational Behavior of CNT-Reinforced Composite Beams, Composite Structures, Vol. 125, 2015, pp. 434–448, DOI: 10.1016/j.compstruct.2015.02.033.

[30] Duarte, H. V., Donadon, L. V., and Avila, A. F., Mechanical Properties of Nanocomposite Laminated Structure and its Sensibility to Modal Analysis Procedure, Latin American Journal of Solids and Structures, Vol. 11, No. 2, 2014, pp. 245–259, DOI: 10.1590/S1679-78252014000200006.

[31] Sanliturk, K. Y., Koruk, H., Development and Validation of a Composite Finite Element with Damping Capability, Composite Structures, Vol. 97, 2013, pp. 136–146, DOI: 10.1016/j.compstruct.2012.10.020.

[32] Perez, M. A., Gil, L., Sanchez, M., and Oller, S., Comparative Experimental Analysis of the Effect Caused by Artificial and Real Induced Damage in Composite Laminates, Composite Structures, Vol. 112, 2014, pp. 169–178, DOI: 10.1016/j.compstruct.2014.02.017.

[33] Perez, M. A., Gil, L., and Oller, S., Impact Damage Identification in Composite Laminates Using Vibration Testing, Composite Structures, Vol. 108, 2014, pp. 267–276, DOI: 10.1016/j.compstruct.2013.09.025.

[34] Herman, A. P., Orifici, A. C., and Mouritz, A. P., Vibration Modal Analysis of Defects in Composite T-Stiffened Panels, Composite Structures, Vol. 104, 2013, pp. 34–42, DOI: 10.1016/j.compstruct.2013.04.012.